Appendix E

Supplementary results with Figure S5 - Figure S12 and Table S1

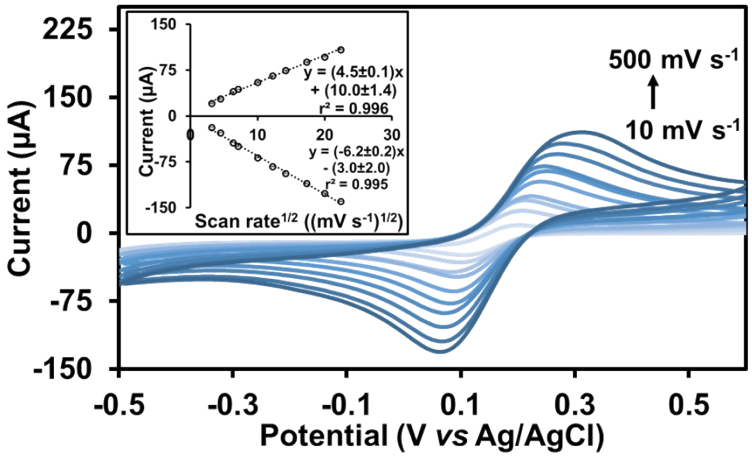

Fig. S5. Cyclic voltammograms of 6 mmol L^{-1} $K_3Fe(CN)_6$ in 0.1 mol L^{-1} KCl obtained from the "planar-disc gold leaf sensor" at various scan rates (10, 20, 40, 50, 100, 150, 200, 300, 400 and 500 mV s^{-1}). The plots of the anodic current and cathodic current against the square root of the scan rate are shown as inset.

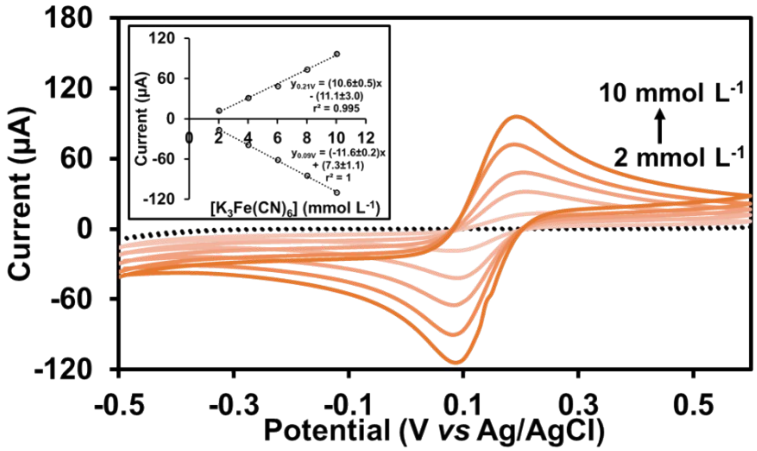

Fig. S6. Performance of the "planar-disc gold leaf sensor" in analyzing samples as droplet (100 µL) showing the cyclic voltammograms of 2-10 mmol L^{-1} $K_3Fe(CN)_6$ in 0.1 mol L^{-1} KCl solution. The calibration lines from the oxidation and the reduction peak potentials are shown as inset.

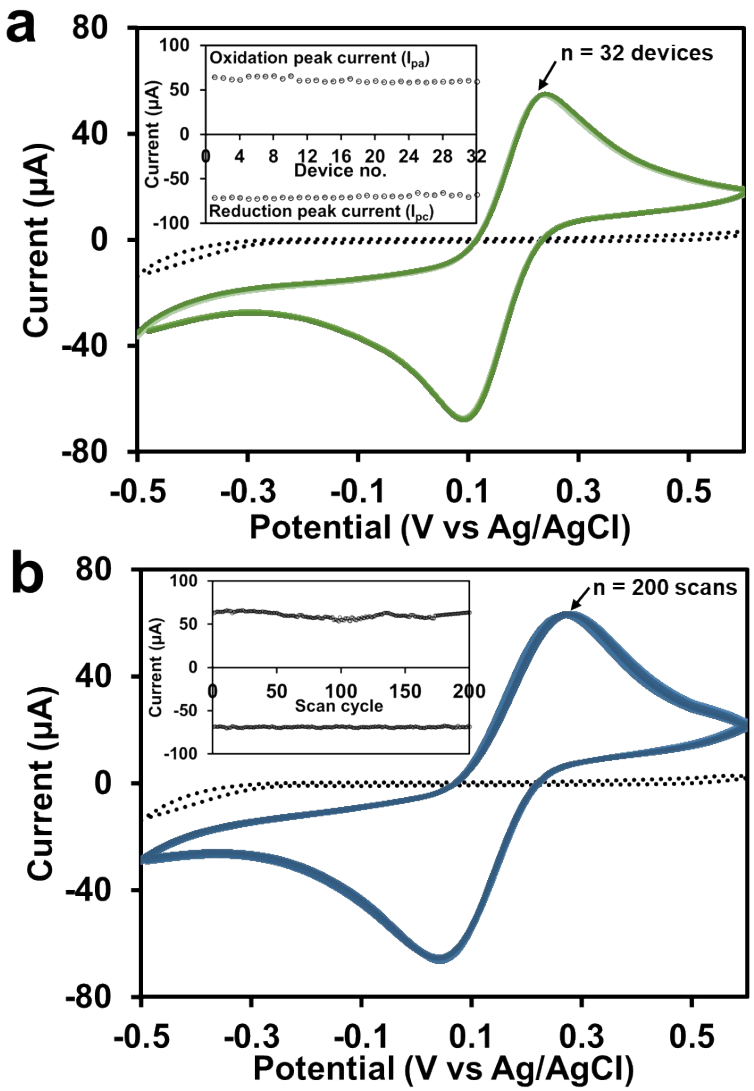

Fig. S7. Cyclic voltammograms of 6 mmol L^{-1} $K_3Fe(CN)_6$ in 0.1 mol L^{-1} KCl (dark lines) obtained from the planar-disc gold leaf sensors in the tests of (a) fabrication reproducibility: 96 CV scans of 32 different sensors (triplicate scans per sensor) and of (b) reusability of the sensor: 200 scan-cycles of a single sensor. Each inset presents the values of I_{pa} and I_{pc} obtained from each set of the CV scans. Dotted lines are the background signals for 0.1 mol L^{-1} KCl.

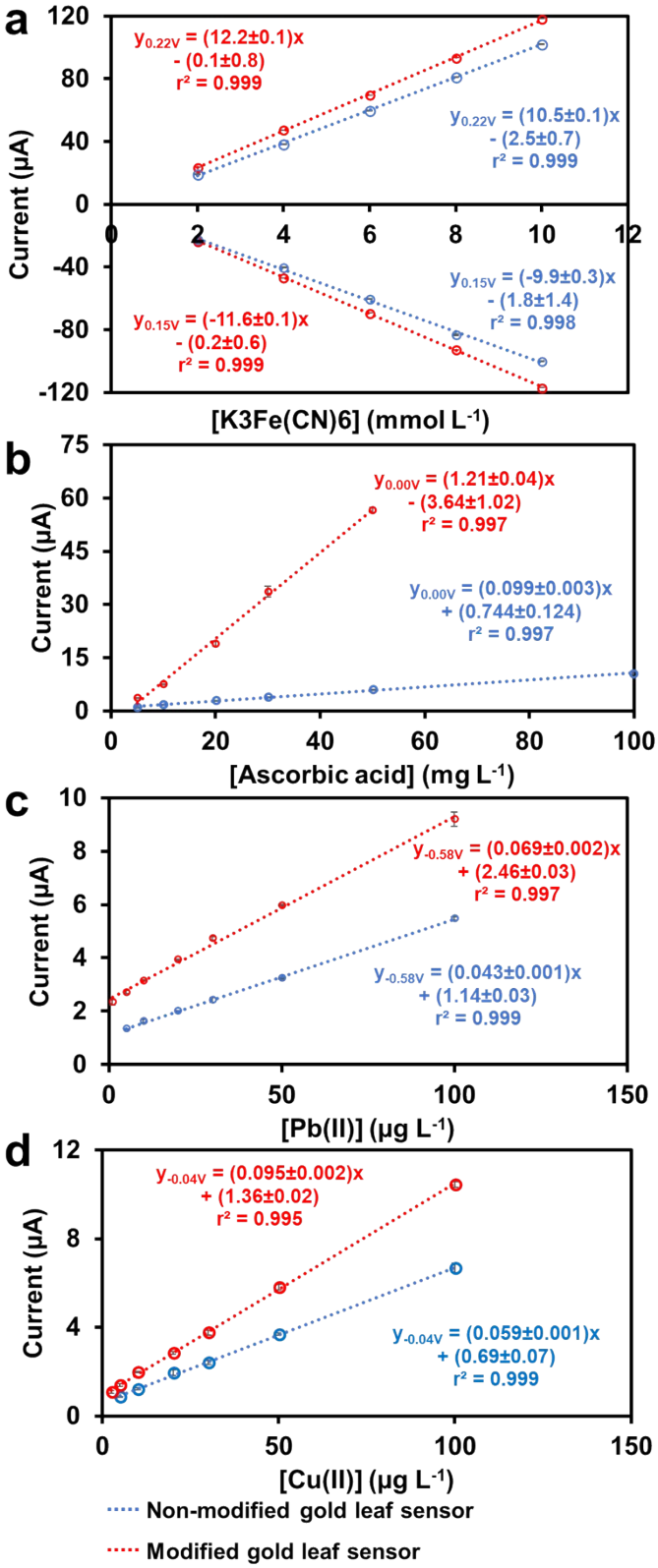

Fig. S8. Examples of increase in sensitivities after surface modification of planar-disc gold leaf surface: (a) quantitation of ferricyanide by cyclic voltammetry, (b) determination of ascorbic acid by square wave voltammetry and analysis of (c) Pb(II) and (d) Cu(II) by square wave anodic stripping voltammetry.

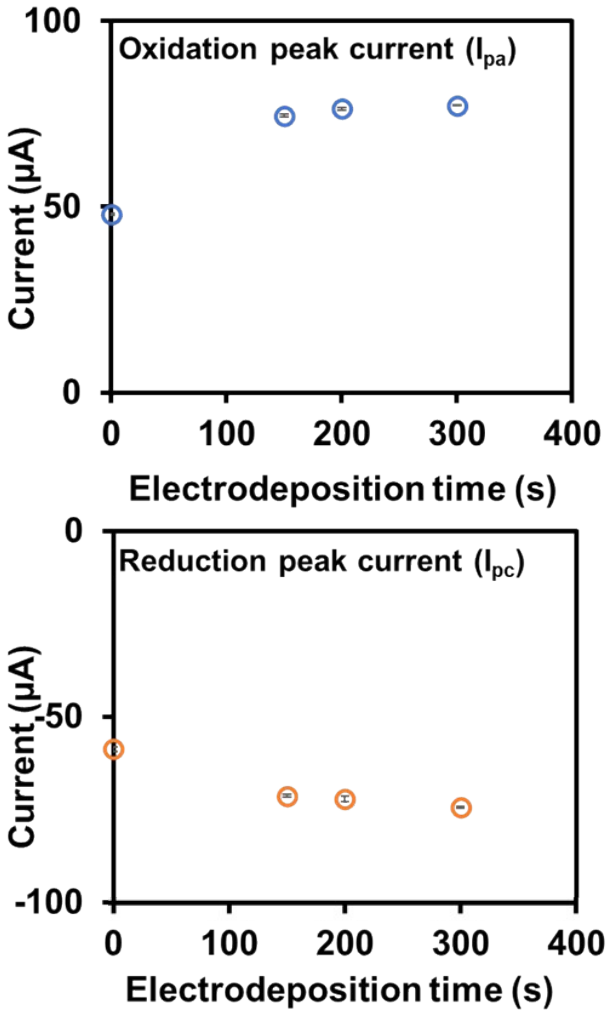

Fig. S9. Effect of electrodeposition time on the property of the "planar-disc gold leaf sensor". The currents are from repetitive scans of cyclic voltammograms using the test ferricyanide solution (6 mmol L^{-1} $K_3Fe(CN)_6$ in 0.1 mol L^{-1} KCl).

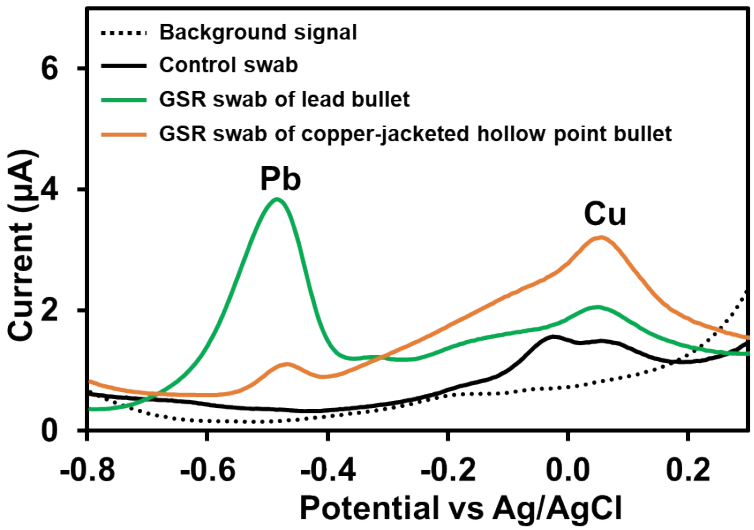

Fig. S10. Voltammograms from SWASV of the extracts from swabs of GSR at bullet holes and periphery of the holes after firing a single lead or copper-jacketed hollow point bullet. The control is the extract of the swab taken from zinc metal sheet target before firing. The background is the voltammogram of the supporting electrolyte.

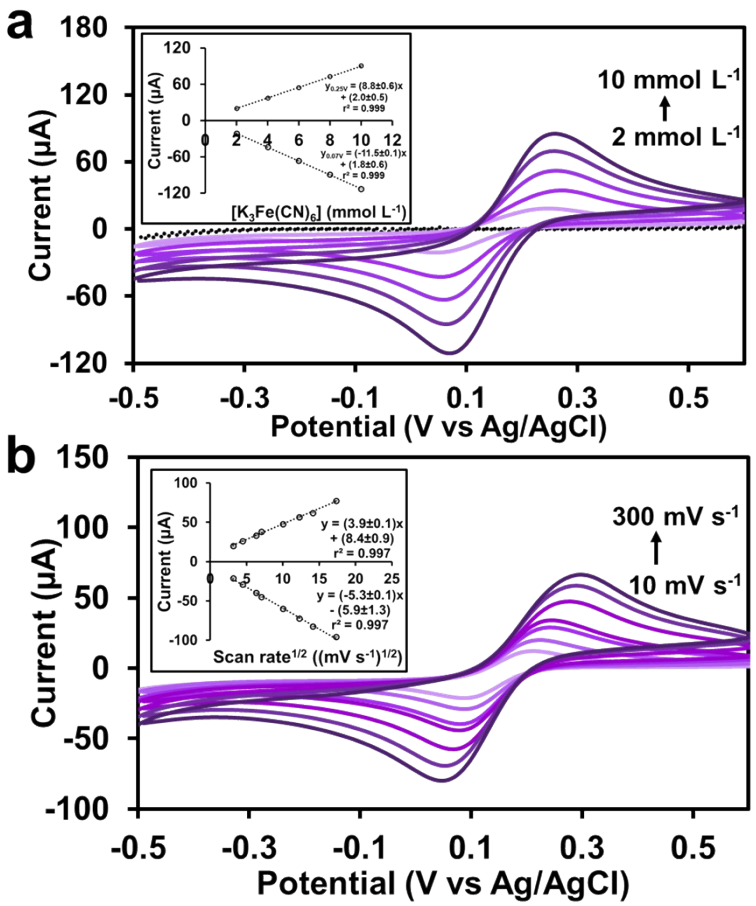

Fig. S11. Characterization of the planar gold leaf with hand-drawn carbon and silver-silver chloride electrodes by (a) CV scans in 2-10 mmol L-1of $K_3Fe(CN)_6$ solutions in 0.1 mol L^{-1} KCl with the calibration graphs in the inset and (b) the effect of scan rate investigated using 6 mmol L^{-1} of $K_3Fe(CN)_6$ solution in 0.1 mol L^{-1} KCl.

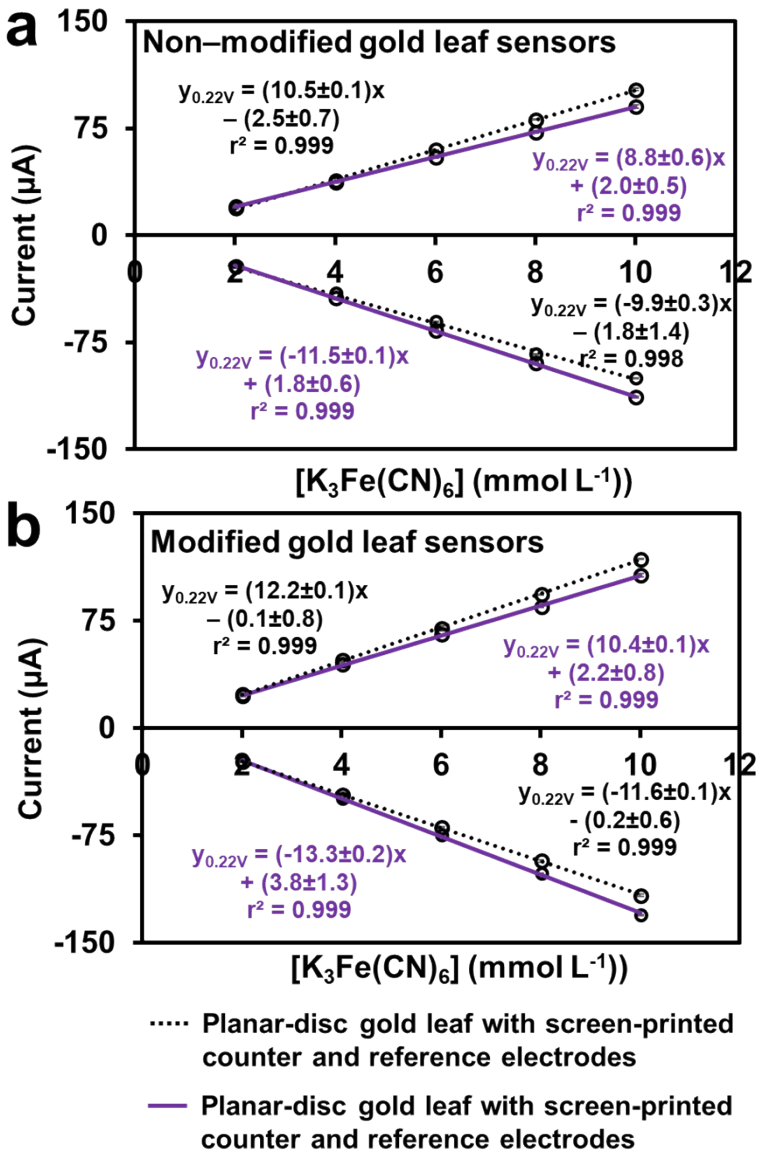

Fig. S12. Plots of the anodic or cathodic peak current against concentration of ferricyanide obtained from the characterizations of the hand-drawn sensor and the screen-printed sensor before and after the gold electrodeposition process on gold leaf surfaces.

Table S1. Determination of Pb(II) in bottled drinking water and bottled mineral water and recovery of spiked samples using the "planar-disc gold leaf sensor"

Sample	Pb(II) contents (μg L^{-1}) (n=3)			%Recovery
	Measured	Added	Found	
Bottled drinking water #1	n.d.	20.0	20.5 ± 0.6	102 ± 3
Bottled drinking water #2	n.d.	20.0	20.7 ± 0.2	103 ± 1
Bottled mineral water #1	n.d.	20.0	20.7 ± 0.8	104 ± 4
Bottled mineral water #2	n.d.	20.0	20.2 ± 0.8	101 ± 4

n.d. = not detectable, LOD = 3.2 μg L^{-1}